Effects of Hybrid Exchange Correlation Functional (Vwdf3) on the Structural, Elastic, and Electronic Properties of Transition Metal Dichalogenides

S. A. Yamusa[a], A. Shaari[b], I. Isah[c], U. B. Ibrahim[d], S. I. Kunya[c], S. Abdulkarim[d], Y. S. Itas[e,*], I. M. Alsalamh[f]

[a] *Department of Physics, Federal College of Education Zaria, P.M.B 1041, Zaria, Kaduna State, Nigeria*
[b] *Department of Physics, Faculty of Science, Universiti Teknologi Malaysia*
[c] *Department of Science Laboratory Technology, Jigawa State Polytechnic, Dutse, Jigwa State Nigeria*
[d] *Faculty of Science, Physics Department Kano University of Science and Technology, Wudil, Kano, Nigeria*
[e] *Department of Physics, Bauchi State University, Gadau, P.M.B. 65 Bauchi, Nigeria*
[f] *Physics Department, Faculty of Science, University of Hail, Saudi Arabia*

Abstract

In this research, the effects of Van der Waals forces on the structural, elastic, electronic, and optical properties of bulk transition metals dichalcogenides (TMDs) were studied using a novel exchange-correlation functional, vdW-DF3. This new functional tries to correct the hidden Van der Waals problems which are not reported by the previous exchange functionals. Molybdenum dichalcogenide, MoX_2 (X = S, Se, Te) was chosen as a representative transition metal dichalcogenide to compare the performance of the newly designed functional with the other two popular exchange-correlation functional; PBE and rVV10. From the results so far obtained, the analysis of the structural properties generally revealed better performance by vdW-DF3 via the provision of information on lattice parameters very closer to the experimental value. For example, the lattice constant obtained by vdW-DF3 was 3.161 Å which is very close to 3.163 Å and 3.160 Å experimental and theoretical values respectively. Calculations of the electronic properties revealed good performance by vdW-DF3 functional. Furthermore, new electronic features were revealed for MoX2 (x = S, Se, Te). In terms of optical properties, PBE functional demonstrates lower absorption than vdW-DF3, as such it can be reported that vdW-DF3 improves photon absorption by TMDs. However, our results also revealed that vdW-DF3 performed well for MoS2 than for MoSe2 and MoTe2 because of the lower density observed for the S atom in MoS2.

Communicated by: Taoreed Owolabi

1. Introduction

The study of transition metal dichalcogenides has grown in popularity as a condensed matter physics research area and as a potential resource for a range of applications that could

*Corresponding author tel. no: +2348069316888
Email address:* yitas@basug.edu.ng (Y. S. Itas)

affect scientific and high-tech advancement. DFT explanations on how electrons in the many-body systems interact with each other depending on the so-called approximations of the exchange-correlation (XC) functional [1]. Moreover, much of the successes in DFT came from the fact that these functions often produce accurate results. However, there are some situations where failures are reported by many of these functional [2]. Therefore, there is a need to understand the accurate XC functional to adequately describe the behavior of the many-body electronic system. One good example of failure by XC is the inability to fully describe a long-range electron interaction also called dispersion forces. Van der Waals problem by local density approximation (LDA) and Perdew-Burke-Ernzerh (PBE) exchange functional remains a challenge that needs urgent improvement [3] The problem of lack of dispersion forces otherwise referred to as van der Waals (vdW) forces, is one of the most disturbing problems in DFT.

Therefore it becomes one of the most traded topics in condensed matter physics and material science. It can be understood by the fact that over 800 dispersion-based DFT studies were reported in 2011 compared to fewer than 80 in the whole of the 1990s [4]. Recent studies have revealed that LDA exhibits overestimations of the lattice constants for a and c of 0.4 % and 5.2 %, and GGA underestimates c by 4 % while overestimating a by 0.58 %, respectively. This problem persisted in TMDs, especially in terms of their mechanical, electronic, and optical characteristics [5]. In this research, a full demonstration of the effects of Van der Waals forces on the mechanical, electronic, and optical properties of TMDs was carried out with MoX_2 (X = S, Se, and Te).

Transition metal dichalcogenides are types of materials that can be metallic or semiconducting [6]. The semiconducting TMDs represent the layered materials [7], they can also be classified as direct or indirect energy band gap materials. For example, MoS_2, $MoSe_2$, WS_2, and WSe_2 are direct band gap semiconductors.

In this study MoS_2, $MoSe_2$ and $MoTe_2$ were considered. Molybdenum dichalcogenides MoX_2 (X = S, Se, and Te) in the most stable phase 2H-MX2 belong to the space group P63/mmc (194), it has a hexagonal crystal structure with Wyckoff positions of 2c and 4f with z coordination value of 0.3779. Literature studies revealed that the study of the effect of Van der Waals forces on this material using the new exchange functional vdW-DF3 has not been conducted. Although MoS2 has been reported as good material for hydrogen storage [8], there are need to explore the potentials of other di-chalcogenides such as MoSe2 and MoTe2. Based on the obtained results, vdW-DF3 may demonstrate promising results on the electronic and optical properties of TMDs. Table 1 demonstrates the results on the effect of the pre-existing exchange functional with the experimental values. Reports from Table 1, revealed that there are still more problems to solve regarding the effect of Van der Waals, for example, the obtained value for the lattice parameter with PBE is 3.680 Å, that of rVV10 is 2.186 Å which is far away from the experimental value of 3.163 Å obtained.

Therefore there is a need to use better exchange functional such as vdW-DF3 for better improvement in the next generations' sustainability science and technology to pave way for optoelectronic applications.

2. Research Method

The three materials were first optimized using three selected exchange-correlation functional (PBE, rVV10, and vdW-DF3) by setting the Brillouin zone sample $12 \times 12 \times 3$ Monkhorst Pack k-mesh and 800 eV plane wave cut-off energy. The optimization was performed till the total energy and force converged to 10^{-3} eV, this is true for all three materials (MoS_2, $MoSe_2$, and $MoTe_2$). The calculations were performed via ab initio density functional theory (DFT) using plane-wave basis as implemented in the Quantum-ESPRESSO package, this includes the optimization, and determination of equilibrium lattice parameters, and electronic band gaps. An auxiliary package to the quantum ESPRESSO `thermo_pw` [1] was also used in the calculation of the elastic constants and optical properties. To make an accurate comparison, Kohn-Sham equations were applied by implementing the DFT ab initio quantum computing framework within the Perdiew-Burke-Emzahope (PBE) exchange functional [9], rVV10 and our novel VdW-DF3 functional. Calculations were performed using a non-spin polarized DFT to save computational costs. To ensure accurate results in this study, TMDs were appropriately relaxed to appropriate geometries. For all three systems, the length and the height were chosen as 12.03 Å each. The chiral/translation vectors were constructed such that the maximum force, stress, and displacements were set at 0.05 eV/Å each.

3. Results and Discussion

3.1. Structural and Elastic Properties

The equilibrium lattice parameters for the three systems were determined by fitting energy volume in the standard equation of the state. This can also be obtained by polynomial fit to the energy-volume data [10]. The lattice parameter can be determined from equilibrium volume as:

$$a_0 = \left(\frac{V}{K}\right)^{1/3} \tag{1}$$

where K is the ratio c/a for the materials MoX_2 (X = S, Se, and Te). The crytallogrphic structure of MoS_2, $MoSe_2$ and $MoTe_2$ are presented in Figure 1.

The lattice parameters were calculated such that the three systems can be viewed as having a hexagonal P6_3/mmc symmetry with a lattice constant of 3.66 Å. The Mo-S and S-S bond lengths are 2.415 Å and 3.131 Å respectively which agrees with the available literature [11]. In the case of MoSe2, the bond lengths of Mo-Se and Se-Se atoms were 2.424 Å and 3.113 Å, respectively. To obtain significant results from our calculations,
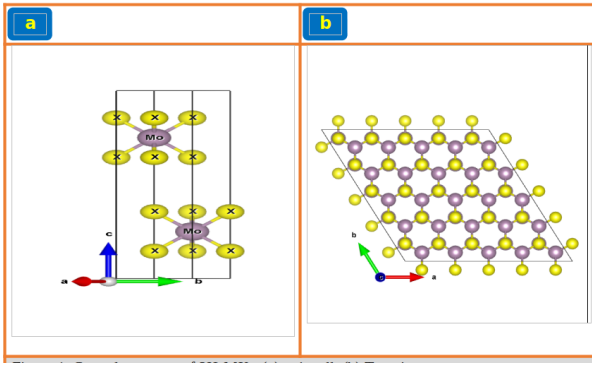
Figure 1: Crystal structure of 2H-MX$_2$: (a) unit cell, (b) Top view

$$C_{11} > |C_{12}| \tag{2}$$

$$2C_{13}^2 < C_{33}(C_{11} + C_{12}) \tag{3}$$

$$C_{44}, C_{66} > 0, \tag{4}$$

where $C_{66} = (C_{11} - C_{12})/2$ and C_{ij} are the five independent elastic constants for the hexagonal materials.

As presented in Table 2, VdW-DF3 revealed high mechanical stability for all systems. Therefore it can be reported that VdW-DF3 XC functional significantly improves correction to Van der Waals problem in TMDs.

3.2. Electronic Properties

The electronic band structures of the Molybdenum chalcogenides MoX$_2$ (X = S, Se, Te) were calculated along the high symmetry point of the Brillouin zone by following the k- paths $\Gamma - M - K - \Gamma$ for all the three systems. Results of the three XC functional (PBE, rVV10 and vdW-DF3) were obtained as presented in Figure 2. The valence band maximum (VBM) and conduction band minimum (CBM) located at Γ and between $\Gamma - K$, respectively, were used to determine the band gaps as shown in Table 3.

To further explain the efficiency of VdW-DF3 XC functional, the electronic band structure and density of states were calculated for MoS$_2$, MoSe$_2$ and MoTe$_2$ systems, the results presented in Figure 2 show that MoS$_2$ demonstrated band gap of 0.79 eV, MoSe 2 revealed 0.88 eV and MoTe$_2$ was found to be 0.67 eV. This results showed significant improvement in narrowing the band gap of TMDs by vdW-DF3 XC functional which brought them to new applications for optoelectronics [25]. Therefore vdW-DF3 XC functional make significant contribution towards turning TMDs from wide gap to narrow gap semiconductors. In terms the partial density of states (PDOS), calculations were performed to determine contributions by different s, p, d, f orbitals, the results are illustrated in Figure 2 (b, d and f).

lattice parameters of MoTe2 were also studied, these were ensured to be 2.423 Å and 3.116 Å respectively. To further understand the vdW-DF3 effects, we calculated the formation energy based on the lattice parameters earlier reported [12, 13]. The results are presented in Table 2. The result predicted the output of the effects of Van der Waals under PBE, rVV10, and the novel vdW-DF3 exchange functional. Table 1 presented the result of the calculated equilibrium lattice parameter of Molybdenum Chalcogenide MoX2 for the three exchange-correlation functional (PBE, rVV10, and vdW-DF3) compared to the available experimental and theoretical results.

Table 1: The calculated lattice parameters with the three functional are compared with the available experimental and theoretical results

		PBE (Å)	rVV10 (Å)	VdW-DF3 (Å)	Theor. results [15] (Å)	Expt.	Ref.
MoS$_2$	a(Å)	3.680	2.186	3.161	3.163	3.160	[14]
	c(Å)	13.37	13.394	12.296	12.442	12.290	[16]
MoSe$_2$	a(Å)	2.314	3.523	3.293	3.295	3.288	[17]
	c(Å)	13.001	13.036	12.918	13.088	12.920	[18]
MoTe$_2$	a(Å)	3.874	3.489	3.551	3.617	3.520	[19]
	c(Å)	13.906	13.965	13.817	14.261	13.970	[11]

It can be seen that the vdW-DF3 successfully describe accurately the lattice parameter of the three systems with only 1 % error. This shows that the functional performed excellently in the determination of the lattice parameters of a bulk MoX$_2$.

Molybdenum chalcogenide MoX$_2$ (X = S, Se, Te) is a hexagonal crystal with 2H-MoX$_2$ as the most stable phase. For this type of crystal, there are only five independent elastic constants. The five elastic constants were used to check the stability of the optimized structure using the Born stability criteria [20] and to determine the Mechanical properties of the materials for the three correlation functional. The calculated properties were compared with the available literature both experimentally and theoretically [21, 22, 23], which is presented in Table 2. The Born stability criteria were checked using equations (2) - (4 [24).

To further elaborate on the nature of the band gap of the three systems, the total density of State (TDOS) and partial density of state for the MoS$_2$, MoSe$_2$, and MoTe$_2$, are illustrated in Figure 2. In terms of MoS$_2$ (Figure 2(b)), the lower valance bands at -6.95 to 0.28 eV are composed mainly of Mo-4d states and S-3p states, zero states were seen from 0.28 to 0.58 eV. The conduction bands are mainly due to Mo-4d and S-3p states located at 0.68 to 3.92 eV, there are lower contributions above 4.002 eV up to the conduction bands. For MoSe$_2$ (Figure 2(d)), the valance bands are composed of Mo-4d and Se-4p states located at -5.99 to 0.24 eV, the width 0.47 eV to 0.0.36 eV is the Fermi level of zero states and above 0.35 eV is mainly composed of Mo-4d and Se-4p states for conduction bands. For MoTe$_2$, valance band contribution starts from the energy range of -5.69 to 0 eV mainly by Mo-4d Te-5p states, Fermi level was show from 0 eV to 0.2 eV, and the conduction bands contribution is the energy range above 0.74 eV mainly by Mo-4d and Te-5p. it can beseen that vdW-DF3 was able to

Table 2: Elastic constants in Gpa, Bulk Modulus B in Gpa, Young modulus E in Gpa, and Shear Modulus G in Gpa For three functional for MoX$_2$, (X = S, Se, and Te)

Material	Funct.	C_{11}	C_{12}	C_{13}	C_{33}	C_{44}	B	G	E	B/G	σ
	PBE	214.39	51.92	13.43	55.27	17.73	57.860	97.784	40.13	1.442	0.218
MoS$_2$	rVV10	218.01	53.89	18.86	69.27	4.48	65.303	73.342	27.933	2.338	0.313
	vdW-DF3	94.21	76.71	25.85	305.07	5.00	79.171	50.102	17.964	4.407	0.395
	PBE	78.34	64.68	46.85	403.90	2.36	83.32	83.698	47.07	1.046	5.001
MoSe$_2$	rVV10	88.32	68.71	53.27	387.93	3.53	88.38	89.207	50.233	1.118	4.994
	vdW-DF3	87.94	69.88	47.15	459.24	4.31	91.39	91.845	58.691	1.495	4.361
	PBE	116.84	30.71	36.83	111.78	25.16	61.577	85.590	33.741	1.825	0.268
MoTe$_2$	rVV10	119.70	33.14	20.33	69.05	26.98	48.538	82.769	34.039	1.426	0.216
	vdW-DF3	122.44	31.08	13.33	54.48	27.91	42.193	82.021	34.873	1.210	0.176

Figure 2: Electronic band structure and density of state of MoS$_2$ (a) and (b), MoSe$_2$ (c) and (d), and (e) and (f) for MoTe$_2$ using three the fuctionals

Table 3: The energy gap of MoS$_2$, MoSe$_2$, and MoTe$_2$ with the three exchange-correlation functionals

System	PBE (eV)	rVV10 (eV)	vdW-DF3 (eV)	Ref.
MoS$_2$	0.84	0.85	0.79	This work
MoSe$_2$	0.84	0.75	0.88	This work
MoTe$_2$	0.73	0.67	0.67	This work

figure out all orbitals contributions as against PBE and rVV10 XC functionals.

3.3. Optical Properties

The optical properties of Mos$_2$, MoSe$_2$, and MoTe$_2$ bulk crystals with polarization along x-direction (in-plane) are calculated using independent particle approximation by solving time-dependent density-functional theory (TDDFT) and linear response technique [3], using the Sternheimer approach within `Thermo_ pw` code [1], a proprietary branch of the quantum ESPRESSO project [4]. The calculated real and imaginary parts of frequency-dependent microscopic dielectric function in the energy range of 0 to 21 eV were plotted. The imaginary parts of the dielectric function of MoS$_2$ (Figure 4), MoSe$_2$ (Figure 5), and MoTe$_2$ (Figure 6) were obtained from interband transition for the parallel and perpendicular direction of the electric field as computed from equation (3) [5], however, the real part of the frequency-dependent dielectric function was obtained from Kramers-kroning relation as shown in equation (6) [2]:

$$\epsilon_2(\omega) = \frac{2\pi e^2}{\Omega \epsilon_0} \Sigma_{\kappa,\nu,c} \left\| \bar{\lambda}. \left\langle \psi_k^c | u.r | \psi_k^\nu \right\rangle \right\|^2 \delta \left(E_k^c - E_k^\nu - E \right). \quad (5)$$

where $\bar{\lambda}$ is the polarization vector of light and the integral is over the Brillouin zone, u, ω, e, ψ_k^c, ψ_k^ν are the polarization vector of the incident electric field, frequency of light, the electronic charge, and conduction and valance band wave function at k, respectively.

$$\epsilon_1(\omega) = 1 + \frac{2}{\pi} P \int_0^\infty \frac{\omega' \epsilon_2(\omega')}{\omega'^2 - \omega^2} \, d\omega', \quad (6)$$

where P denotes the integral's principle value. The computed real and imaginary dielectric functions of MoS$_2$, MoSe$_2$, and
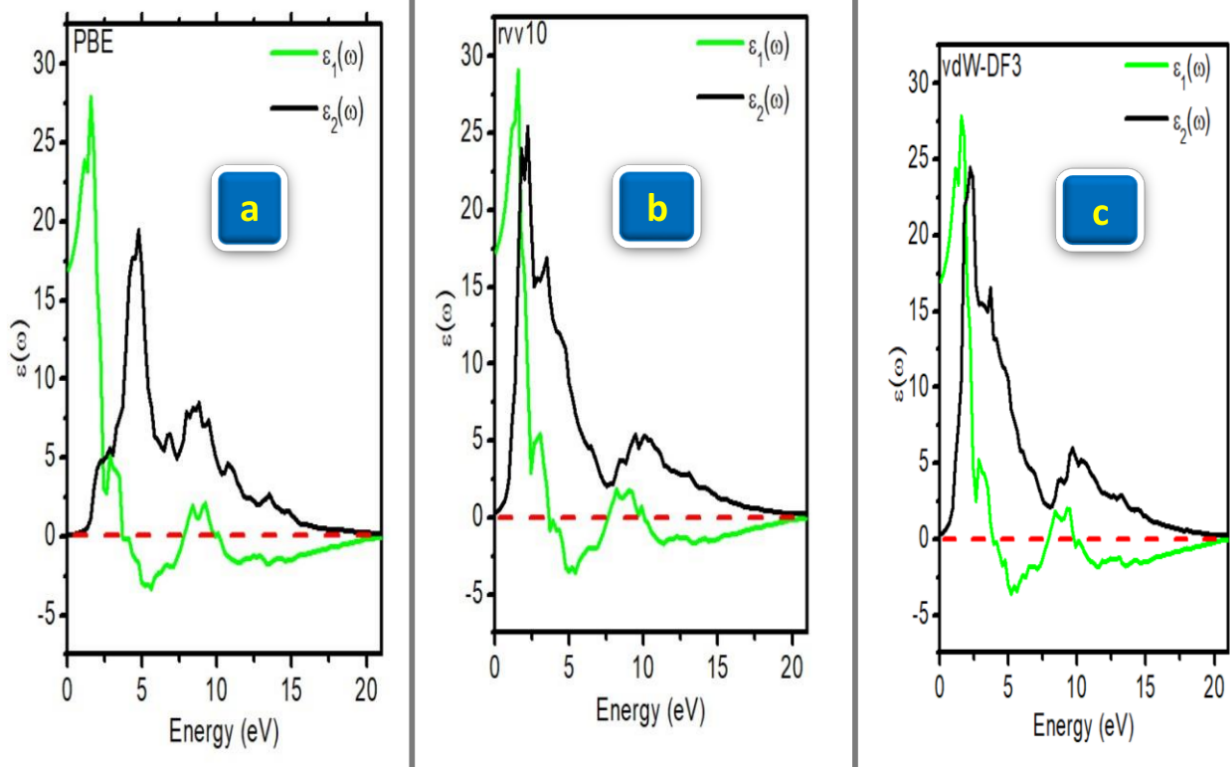
Figure 3: Real and imaginary dielectric functions for MoS_2 with respect to the (a) PBE (b) rVV10 and (c) vdW-DF3 functionals
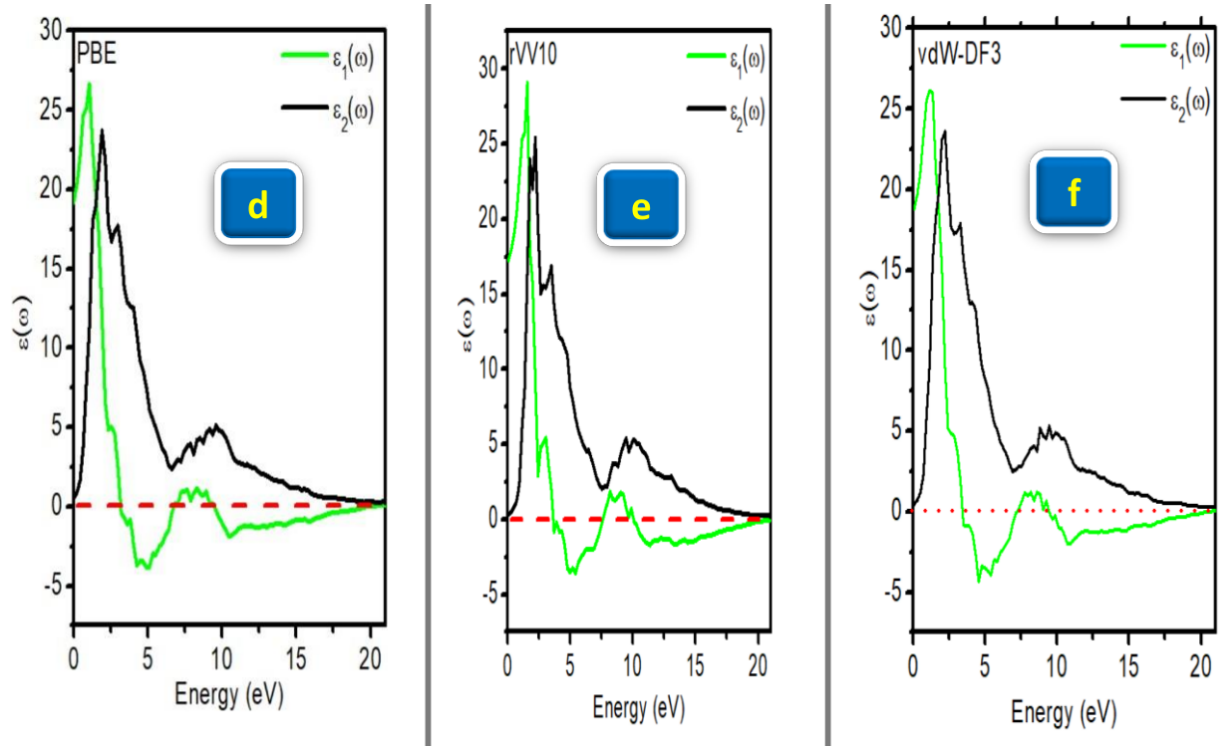
Figure 4: Real and imaginary dielectric functions for $MoSe_2$ with respect to the (d) PBE (e) rVV10 and (f) vdW-DF3 functionals

$MoTe_2$ within the three functionals are plotted in Figures 3, 4 and 5, respectively. The result shows that the interband transition due to Mo-4d and S-3p, Se-4p, and Te-5p states move to lower energies from MoS_2, $MoSe_2$, and $MoTe_2$, respectively. Both MoS_2, $MoSe_2$ and $MoTe_2$ materials show anisotropy [8] in the energy range from 0 to 7.5 eV and isotropy at higher
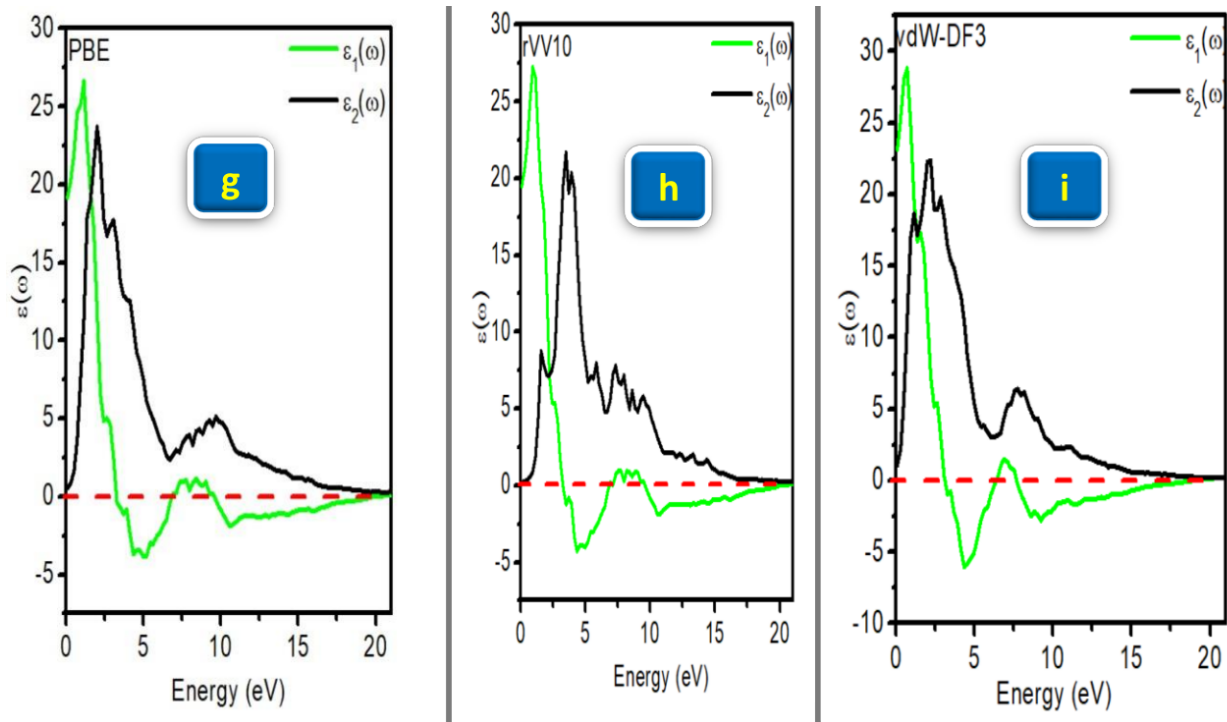
Figure 5: Real and imaginary dielectric functions for MoTe$_2$ with respect to the (a) PBE (b) rVV10 and (c) vdW-DF3 functionals

energy.

To further confirm the band gap in the three systems, a bound state can be seen at 2.0 eV, 1.1 eV and 1.2 eV for PBE, rVV10 and vdW-DF3 functional respectively, the results obtained by vdW-DF3 was found to be in good agreement with previous theoretical results [15]. Similar results were also obtained for MoSe$_2$, MoTe$_2$, these were presented in Figures 4 and 5, respectively.

To describe optical absorption, the imaginary dielectrics for all systems were studied. Favourable results were obtained by vdW-DF3 functional, for example higher optical absorptions were observed for MoS$_2$ (Figure 3c) at 22.5 cm^{-1} which corresponds to 2.80 eV, this is the absorption in the visible range, other functionals only demonstrated absorption in the infra-red range, which significantly underestimates the absorption characteristcs of TMDs.

4. Conclusion

To conclude this work, results so far obtained brought out new hidden properties of TMDs which failed to be reported by PBE and rvv10 functionals. Calculation of the elastic properties revealed that TMDs are more stable with vdW-DFT3, higher moduli of elasticity such as Young's Moduli, shear moduli and bulk moduli were significantly improved with well agreement with theoretical results. From the results of electronic properties, it revealed that bulk TMDs can be turned from being a wide gap semi conductors to being a narrow gap semiconductors, it also shows that d'orbital majorly contributed to narrowing the band gap in all the sysyems. Higher optical absorption are also repoted by vdW-DF3, this brought the systems under study as potential candidates for optoelectronics [25].

References

[1] I. G. Kaplan, Modern State of the Conventional DFT Method Studies and the Limits Following from the Quantum State of the System and Its Total Spin. Density Functional Theory-Recent Advances, New Perspectives and Applications, IntechOpen, (2022).

[2] S. Ghosh & K. Bhattacharyya, "Origin of the Failure of Density Functional Theories in Predicting Inverted Singlet-Triplet Gaps", The Journal of Physical Chemistry A **126** (2022) 1378.

[3] M. Kamiya, T. Tsuneda, & K. Hirao, "A density functional study of van der Waals interactions", The Journal of chemical physics **117** (2002) 6010.

[4] Y. S. Itas, C. E. Ndikilar, & T. Zangina, "Carbon Nanotubes: A Review of Synthesis and Characterization Methods/Techniques", The International Journal of Science & Technology **8** (2020) 43.

[5] M. Smyrnioti & T. Ioannides, "Dimethyl Ether Oxidation over Copper Ferrite Catalysts", Catalysts **12** (2022) 604.

[6] S. A. Yamusa, A. Shaari, & I. Isah, "Structural stability, Electronic and Optical Properties of Bulk MoS$_2$ Transition Metal Dichalcogenides: A DFT Approach", J. Appl. Phys. **14** (2022) 40.

[7] S. Chen & Y. Pan, "Mechanism of interlayer spacing on catalytic properties of MoS$_2$ from the ab-initio calculation", Applied Surface Science **599** (2022) 154041.

[8] Y. Pan, "Role of SS interlayer spacing on the hydrogen storage mechanism of MoS_2" International Journal of Hydrogen Energy **43** (2018) 3087.

[9] Y. S. Itas, A. B. Suleiman, C. E. Ndikilar, A. Lawal, R. Razali, M. U. Khandaker, P. Ahmad, N. Tamam, & A. Sulieman, "The Exchange-Correlation Effects on the Electronic Bands of Hybrid Armchair Single-Walled Carbon Boron Nitride Nanostructure", Crystals **12** (2022) 394.

[10] T. Arlt, M. Bermejo, M. A. Blanco, L. Gerward, J. Z. Jiang, J. S. Olsen, & J. M. Recio, "High-pressure polymorphs of anatase TiO_2. Physical Review B **61** (2000) 14414.

[11] M. L. Pereira Júnior, C. M. Viana de Araújo, J. M. de Sousa, R. T. de Sousa Júnior, L. F. Roncaratti Júnior, W. Ferreira Giozza, & L. A. Ribeiro Júnior, "On the elastic properties and fracture patterns of MoX_2 (X= S, Se, Te) membranes: a reactive molecular dynamics study",Condensed Matter **5** (2020) 73.

[12] Y. S. Itas, A. B. Suleiman, C. E. Ndikilar, A. Lawal, R. Razali, I. I. Idowu, M. U. Khandaker, P. Ahmad, N. Tamam, & A. Sulieman, "Computational Studies of the Excitonic and Optical Properties of Armchair SWCNT and SWBNNT for Optoelectronics Applications", Crystals **12** (2022) 870.

[13] S. A. Yamusa, A. Shaari, N. A. M. Alsaif, I. M. Alsalamah, I. Isah, & N. Rekik, Elucidating the Structural, Electronic, Elastic, and Optical Properties of Bulk and Monolayer MoS_2 Transition-Metal Dichalcogenides: A DFT Approach. ACS omega (2022).

[14] N. Yedukondalu, V. D. Ghule, & G. Vaitheeswaran, "Computational study of structural, electronic, and optical properties of crystalline NH_4N_3", The Journal of Physical Chemistry C **116** (2012) 16910.

[15] S. Chen, Y. Pan, D. Wang, & H. Deng, "Structural stability and electronic and optical properties of bulk WS2 from first-principles investigations", Journal of Electronic Materials **49** (2020) 7363.

[16] I. Diez-Perez, Z. Li, S. Guo, C. Madden, H. Huang, Y. Che, X. Yang, L. Zang, & N. Tao, " Ambipolar transport in an electrochemically gated single-molecule field-effect transistor", ACS Nano **6** (2012) 7044.

[17] B. S. Kim, J.W. Rhim, B. Kim, C. Kim, & S. R. Park, "Determination of the band parameters of bulk 2H-MX2 (M=Mo, W; X= S, Se) by angle-resolved photoemission spectroscopy", Scientific reports **6** (2016) 1.

[18] B. E. McCandless & K. D. Dobson, "Processing options for CdTe thin film solar cells", Solar Energy **77** (2004) 839.

[19] A. Roy, H. C. P. Movva, B. Satpati, K. Kim, R. Dey, A. Rai, T. Pramanik, S. Guchhait, E. Tutuc, & S. K. Banerjee, "Structural and electrical properties of $MoTe_2$ and MoSe2 grown by molecular beam epitaxy", ACS applied materials & interfaces **8** (2016) 7396.

[20] A. Candan, S. Akbudak, Ugur, & G. Ugur, "Theoretical research on structural, electronic, mechanical, lattice dynamical and thermo-dynamic properties of layered ternary nitrides Ti2AN (A=Si, Ge, and Sn)", Journal of Alloys and Compounds **771** (2019) 664. https://doi.org/10.1016/j.jallcom.2018.08.286.

[21] M. L. Pereira Júnior, C. M. Viana de Araújo, J. M. de Sousa, R. T. de Sousa Júnior, L. F. Roncaratti Júnior, W. Ferreira Giozza, & L. A. Ribeiro Júnior, "On the elastic properties and fracture patterns of MoX_2 (X= S, Se, Te) membranes: a reactive molecular dynamics study", Condensed Matter **5** (2020) 73.

[22] L. Wei, C. Jun-fang, H. Qinyu, & W. Teng, "Electronic and elastic properties of MoS2", Physica B: Condensed Matter **405** (2010) 2498. https://doi.org/10.1016/j.physb.2010.03.022.

[23] J. N. Yuan, Y. Cheng, X. Q. Zhang, X. R. Chen, & L. C. Cai, "First-principles study of electronic and elastic properties of hexagonal layered crystal MoS2 under pressure", Zeitschrift fur Naturforschung - Section A Journal of Physical Sciences **70** (2015) 529. https://doi.org/10.1515/zna-2015-0102.

[24] F. Mouhat & F.-X. Coudert, "Necessary and sufficient elastic stability conditions in various crystal systems", Physical review B **90** (2014) 224104.

[25] E. E. Etim, M. E. Khan, O. E. Godwin, & G. O. Ogofotha, "Quantum Chemical Studies on C4H4N2 Isomeric Molecular Species", Journal of the Nigerian Society of Physical Sciences **3** (2021) 429.